energies

MDPI

Article

Thermo-Hydraulic Performance of Multiple Channels and Pin Fins Forming Convergent/Divergent Shape

Mohamad Ziad Saghir

Department of Mechanical and Industrial Engineering, Toronto Metropolitan University, Toronto, ON M5B 2K3, Canada; zsaghir@ryerson.ca

Abstract: Heat enhancement has been addressed by studying flow in channels with different shapes. The present paper investigates a particular channel shape with divergent and convergent forms. Two configurations are addressed: wall channels and pin-fin walls forming divergent/convergent shapes. The flow is assumed to be in a laminar and steady-state condition. The numerical model investigated the heat enhancement for different flow rates represented by Reynolds numbers. The average Nusselt number and the performance evaluation criterion revealed that wall channels outperformed the pin-fin shape. The performance evaluation criterion is higher than 1 for the wall channels. The main reason for this is that the flow passes through and above the wall creating mixing. This flow configuration happened since the wall height is shorter than the test cavity height. It is important to emphasize that pin-fins forming convergent channels did not improve heat enhancement when compared to convergent channels. No significant variation in the pressure drop was detected.

Keywords: convergent/divergent channel; pin fins; heat enhancement; laminar flow

check for updates

Citation: Saghir, M.Z. Thermo-Hydraulic Performance of Multiple Channels and Pin Fins Forming Convergent/Divergent Shape. *Energies* **2022**, *15*, 7993. https://doi.org/10.3390/en15217993

Academic Editor: Rafik Belarbi

Received: 13 October 2022
Accepted: 25 October 2022
Published: 27 October 2022

Publisher's Note: MDPI stays neutral with regard to jurisdictional claims in published maps and institutional affiliations.

Copyright: © 2022 by the author. Licensee MDPI, Basel, Switzerland. This article is an open access article distributed under the terms and conditions of the Creative Commons Attribution (CC BY) license (https://creativecommons.org/licenses/by/4.0/).

1. Introduction

Energy storage and heat transfer are essential topics in our day-to-day lives. From cooling batteries, and buildings, to electrical components, the means to cool a system efficiently and effectively is an attractive design parameter to many industries. Similarly, the micro-electronic components used in our devices produce a lot of heat, and there have been studies to enhance the cooling of these IC chips. In addition, harvesting heat and converting it into energy to be used later using phase change material is becoming a common practice in engineering. This paper focuses on the cooling process of microprocessors by optimizing heat transfer through convergent/divergent mini channels and pin-fins channels. There has been much research in this field examining the advantages of heat transfer with heat sinks for IC chips using different fluids. Studies have shown promising results obtained using phase change materials, various working fluids, various design specifications and materials of the heat sink. The use of channels to optimize the heat transfer of microprocessors is a topic of study in cooling applications. Channels are configured in specific arrangements and parameters to maximize heat removal. In addition, the channel wall was replaced with pin fins, thus allowing the flow to circulate more freely.

Srivastava et al. [1] investigated the effects of ribs and cavities on flow and heat transfer in a convergent–divergent-shaped microchannel with a constant heat flux for Reynolds number (Re) ranging from 120 to 900. Convergent–divergent mini channels, ribs, and cavities were quite effective in heat transfer but gradually lost their effectiveness at large values of Re due to a high-pressure penalty. The overall thermal resistance is reduced by up to 40% while keeping the bottom surface temperature relatively uniform. Increasing the Reynolds number leads to enhanced heat transfer by an increase in the average Nusselt number from 15% to 46%.

Later Srivastava and Dewan [2] investigated four unique mini channels: rectangular, rectangular with ribs and cavities, convergent–divergent (CD) and convergent–divergent

with Ribs and Cavities (CD-RC). Overall thermal performance of the CD-RC was observed to be higher in contrast to the other types in terms of the average Nusselt number, which increased from 16% to 40%. Heat transfer will increase due to sturdy fluid mixing and interruption at the boundary layer. Additionally, the thermal resistance would drop rapidly with an increase in Reynolds number. Duryodhan et al. [3] investigated the overall performance of single-phase liquid flow in heated diverging and converging microchannels.

Lee et al. [4] investigated the effects of angled ribs on turbulent heat transfer and friction factors in divergent rectangular channels. Heat transfer and friction elements of totally developed turbulent flow in divergent rectangular channels with parallel angled ribs have been investigated experimentally. Bayomy and Saghir [5] investigated the heat transfer factors, and overall performance of distinctive aluminum heat sinks filled with aluminum foam for an Intel core i7 processor. Different models were investigated, confirming that metal foam can enhance heat removal.

Rahman et al. [6] investigated free convective heat transfer efficiency in Al_2O_3–Cu/water hybrid nanofluid inside a recto-trapezoidal enclosure. This study describes the natural convection flow of Al_2O_3–Cu/water hybrid nanofluid at distinctive concentrations comprising a range of percentages of Al_2O_3 and Cu nanoparticles in a recto-trapezoidal enclosure whose posterior wall is consistently heated.

Yang et al. [7] investigated the flow and thermal modelling of micro/mini-channel heat sinks. An optimization technique for the flow and overall thermal performance of micro/mini-channel heat sinks is developed for water cooling and liquid metal cooling. Mokrani et al. [8] investigated the design of a microchannel, with a rectangular cross-section and large aspect ratio, that approves the characterization of the flow and convective heat transfer underneath unique conditions and makes it viable to vary the hydraulic diameter of the microchannel. Plant and Saghir [9] conducted experimental and numerical work to study heat enhancement in two and three channels configuration using nanofluids. Later Gorzin et al. [10] investigated the use of ribbed maze serpentine mini-channel heat sinks and their effects on heat transfer and fluid flow. It was determined that serpentine mini-channels have higher pressure drops than straight mini-channel.

Xie et al. [11] and Vajravel et al. [12] investigated using a mini-channel heat sink. This study was conducted for a single-phase laminar flow with water as the coolant flowing through small hydraulic tubes. The results conclude that an improved heat transfer performance with a relatively high-pressure drop was achievable when the channel was narrow and deep with a thin bottom and wall thicknesses. Begag et al. [13] investigated the heat transfer and pressure drop in a mini channel with trapezoidal corrugated partitions using air as the working fluid. There have been many findings concluded from this study, such as the heat transfer and pressure drop can be considerably greater by way of the corrugated floor in contrast to the smooth surface. Khoshvaght-Aliabad et al. [14–16] investigated the effects and cooling performance of sinusoidal–wavy mini channel heat sinks (SWMCHS) having a square cross-section. Zhenping Wan et al. [17] examine the flow characteristics of half-corrugated mini channels by comparing corrugated channels to flat channels at different Reynolds numbers. The key finding is that the pressure drops of the half-corrugated channels are lower than the flat bottom counterpart at low Reynolds numbers.

Ho et al. investigated [18] convective heat transfer of nano-encapsulated phase change material suspension in a divergent mini channel heat sink. Sohel et al. [19] used nanofluid coolant (Al_2O_3-H_2O) for cooling electronics with a volume fraction of 0.10–0.25 volume percent. During the experiment, the different flow rate effects were investigated and found to be between 0.50–1.25 L/min with a Reynolds number between 395–989. Ijam et al. [20], used nanofluid with different volume fractions as a coolant for the mini channel. In a copper heat sink with dimensions 20 × 20 mm, Al_2O_3-H_2O and TiO_2-H_2O nanofluids were tested. The results concluded that adding aluminum oxide to water at 4% volume fractions and the dispersion of TiO_2 to the base fluid improved the thermal conductivity by 11.98% and 9.97%, respectively.

Experiments by Ho et al. [21], were conducted with Al_2O_3-water nanofluid instead of distilled water as the coolant in the mini-channel. The mini-channel heat sink contains ten parallel rectangular mini-channels of 50 mm in length, 1 mm in width and 1.5 mm in height for each channel. Hydraulic and thermal performances have been analyzed, and the Reynolds number ranged from 133 to 1515. The nanofluid showed significant improvement in heat transfer performances compared to distilled water, and further experiments were conducted with various pumping power. Additionally, Ho et al. [22,23] conducted an experimental investigation of the cooling performance of Al_2O_3/water nanofluid in a mini-channel heat sink with a layer of microencapsulated phase change material (MEPCM) in the ceiling. Ghasemi et al. [24] compared the heat dissipation performance of nanofluid (Al_2O_3 nanoparticles suspended in water) to water as the coolant in a heatsink. The only drawback to using the nanofluid is an increase in power consumption but with only a small increase in friction compared to water. The experiment by Awais and Kim [25] compared the thermodynamic performance effects header geometry has on straight mini-channel heat sinks. Two mini-channel heat sinks were tested, one optimized and one with conventional header geometries. Nanofluids of three different concentrations and distilled water were investigated as coolants at five different flow rates. It was concluded that the optimized header geometry outperformed the conventional one with minimum base temperatures of 42.6 °C and 45.15 °C, respectively, and a maximum performance gained at increased flow rates of 73% and 62%, respectively.

In the present paper, an attempt is made to study the numerical performance of three and seven convergent/divergent channels when compared to pin-fins convergent/divergent channels shape. Three parameters will be studied in detail: the average Nusselt number, the performance evaluation criterion and the amount of energy extracted from the system. Section 2 will present the problem description, followed by the finite element formulation in Section 3. Section 4 will study the mesh sensitivity, followed by Section 5, which compares the model with experimental data. Results are presented in Section 6, followed by the conclusion in Section 7.

2. Problem Description

In the present paper, a comparison of the thermohydraulic performance between convergent/divergent channels with solid walls and pin-fins walls will be conducted. The model under consideration consists of a test section, an inlet chamber, and an outlet chamber. A bottom heated block is attached to the test section. Figure 1 presents the problem under consideration. Figure 1a illustrates the entire numerical setup, and Figure 1b,c show the model top view with three channels configuration where the test section is displayed. As seen in Figure 1b, the convergent/divergent channel walls are assumed to be made of solid aluminum having a thickness of 1 mm. Three convergent/divergent channels are displayed for this case, noting that seven channel configuration is also studied. In Figure 1c, the channel walls are replaced with cylindrical pin-fins having a diameter identical to the channel wall thickness (i.e., 1 mm). The spacing between the pin fins identified in the figure by "Sp" will be investigated as it affects the flow distribution. Three values of "Sp" will be studied, 10 mm, 5 mm and 3.3 mm, respectively. Table 1 presents the dimensions used in our analysis for the two convergent/divergent channels configuration. As shown, the distance between walls decreases as the number of channels increases since the test section volume remains the same. Figure 1b shows that the test section dimension is a square with a 50 mm by 50 mm base and a height of 12 mm. The inlet and outlet pipe have a radius of 4 mm and a length of 10 mm. The half-circle mixing chamber has a radius of 25 mm and a height identical to the test section area. The heated block has a thickness of 5 mm. The heat flux shown in Figure 1a is applied at the bottom of the heated block. The entire material is made of aluminum.

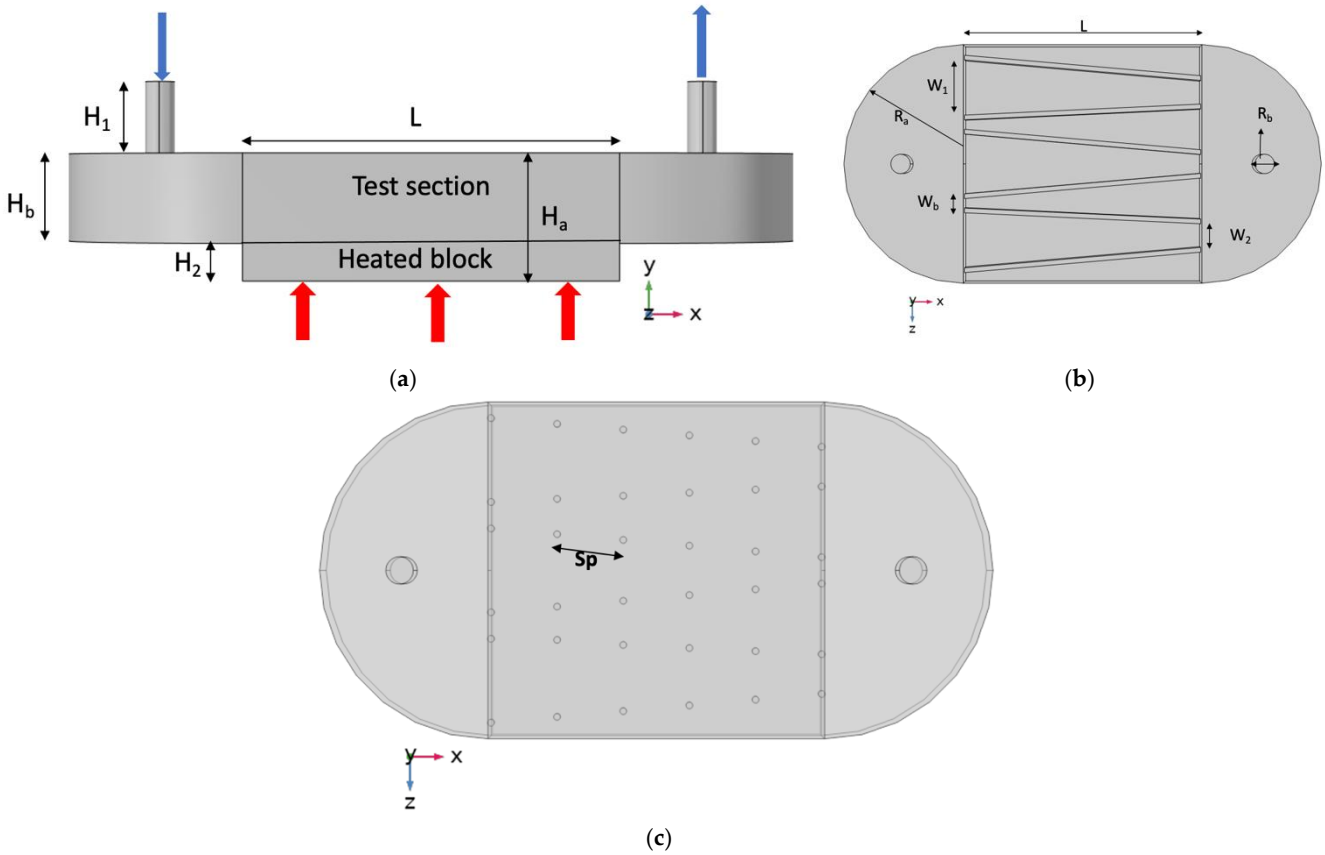


Figure 1. Model under investigation (**a**) Side view, (**b**) convergent channels, (**c**) pin-fins convergent channels.

With such a configuration, the flow accelerates when the fluid enters a wide entrance and decelerates when it penetrates a narrow entrance. Contrary to the channel configuration in the case of pin fins configuration the fluid enters and circulates between the pin-fins before exiting. Thus, no acceleration/deceleration process exists in this case. It is known that an adequate flow rate can extract more heat, and this needs to be confirmed in our analysis. The spacing between the pin-fins will be studied in detail for the best space toward optimum performance.

Table 1. Model dimensions in mm.

Configuration	W_1	W_b	W_2	R_a	R_b	H_a	H_b	H_1	H_2	L
1	12.67	4	6.33	4	4	17	12	10	5	50
2	5.26	1	2.63	4	4	17	12	10	5	50

Multiple channel configurations were investigated, which consist of three channels configuration, shown in Figure 2a and identified as configuration#1. The second case is a seven channels configuration, identified as configuration#2, presented in Figure 2b. In the channel configuration, the channel height varies between 2, 4, 6 and 8 mm; similarly, the pin-fins height varies by 2, 4, 6 and 8 mm, respectively. Thus, the flow circulates between and above the channels and pin-fins. The rationale for this configuration is to minimize the pressure drop in the system.

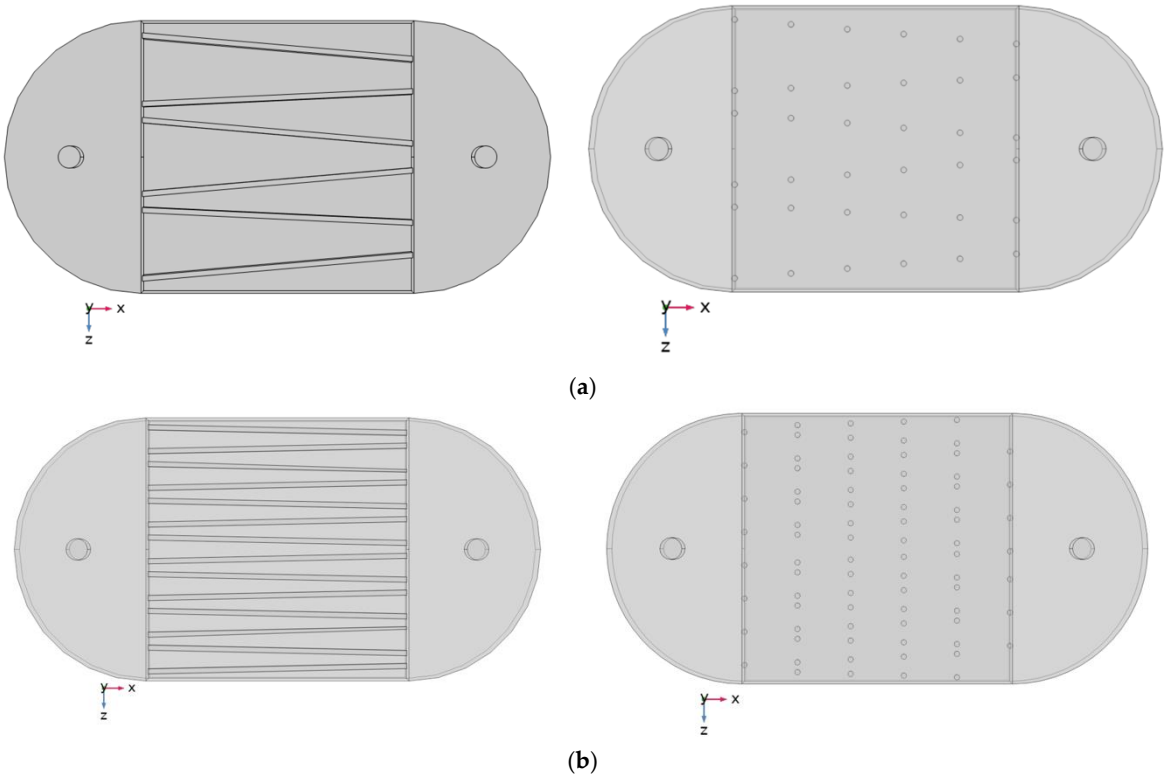


Figure 2. Two configurations under study (**a**) Configuration#1, (**b**) Configuration#2.

3. Finite Element Formulation and Boundary Conditions

Based on the model presented in Figure 1a, the full Navier Stocks equations were solved for the fluid region and the energy equation for the entire model. The flow is assumed Newtonian, which is considered in a laminar regime. Using the following nondimensional variables.

$$X = \frac{x}{D}, Y = \frac{y}{D}, Z = \frac{z}{D}, U = \frac{u}{u_{in}}, V = \frac{v}{u_{in}}, W = \frac{w}{u_{in}}, P = \frac{pD}{\mu u_{in}}, \theta = \frac{(T - T_{in})k}{q'' D} \quad (1)$$

From Equation (1), D is the inlet cylinder diameter, k is the fluid conductivity, and p is the pressure. The inlet velocity is identified by $u_{in,}$ and T_{in} is the inlet temperature.

The fluid flow equations in the three-nondimensional form are as follows:

X-direction

$$Re\left[\frac{\partial U}{\partial \tau} + U\frac{\partial U}{\partial X} + V\frac{\partial U}{\partial Y} + W\frac{\partial U}{\partial Z}\right] = -\frac{\partial P}{\partial X} + \left[\frac{\partial^2 U}{\partial X^2} + \frac{\partial^2 U}{\partial Y^2} + \frac{\partial^2 U}{\partial Z^2}\right] \quad (2)$$

Y-direction

$$Re\left[\frac{\partial V}{\partial \tau} + U\frac{\partial V}{\partial X} + V\frac{\partial V}{\partial Y} + W\frac{\partial V}{\partial Z}\right] = -\frac{\partial P}{\partial Y} + \left[\frac{\partial^2 V}{\partial X^2} + \frac{\partial^2 V}{\partial Y^2} + \frac{\partial^2 V}{\partial Z^2}\right] \quad (3)$$

Z-direction

$$Re\left[\frac{\partial W}{\partial \tau} + U\frac{\partial W}{\partial X} + V\frac{\partial W}{\partial Y} + W\frac{\partial W}{\partial Z}\right] = -\frac{\partial P}{\partial Z} + \left[\frac{\partial^2 W}{\partial X^2} + \frac{\partial^2 W}{\partial Y^2} + \frac{\partial^2 W}{\partial Z^2}\right] \quad (4)$$

In Equation (2) to Equation (4), the nondimensional velocities U, V, and W are in the directions of X, Y and Z, respectively. Here, P is the pressure in nondimensional form, and Re is the Reynolds number. The Reynolds number is defined as $Re = \frac{\rho u_{in} D}{\mu}$.

The energy equation for the fluid portion is as follows

$$\mathrm{RePr}\left[\frac{\partial\theta}{\partial\tau} + \mathrm{u}\frac{\partial\theta}{\partial X} + \mathrm{v}\frac{\partial\theta}{\partial Y} + \mathrm{w}\frac{\partial\theta}{\partial Z}\right] = \left[\frac{\partial^2\theta}{\partial X^2} + \frac{\partial^2\theta}{\partial Y^2} + \frac{\partial^2\theta}{\partial Z^2}\right] \quad (5)$$

Re is the Reynolds number, and Pr is the Prandtl number. The Prandtl number is defined as $\mathrm{Pr} = \frac{C_p\,\mu}{k}$ where C_p is the specific heat of the circulating fluid, μ is the dynamic viscosity, and k is the fluid conductivity. The temperature in the solid part of the model is studied by solving the heat conduction formulation. The boundary conditions applied to this model are as follows

At the inlet

The inlet velocity u_{in} is set equal to 0.025 m/s, 0.05 m/s, 0.0765 m/s, which correspond to a Reynolds number of 100, 200 and 300, respectively.

The inlet temperature T_{in} equals 18 °C, and in the nondimensional form, it becomes equivalent to zero.

At the outlet

The free boundary is applied, and the stresses are equal to zero.

A heat flux q" is applied at the bottom of the test section, and in the nondimensional form, it is set equal to 1.

All external surfaces are assumed insulated, so there are no heat losses. Equations (2)–(5) were solved numerically using the finite element technique. At each iteration, the average relative error of the velocities, pressure and temperature are computed, respectively. Convergence is reached if the residue for all unknowns is below 1×10^{-6} in two successive iterations.

This analysis will investigate three variables to determine the structure shape's importance. The first nondimensional term is the Nusselt number which will be evaluated at the base of the channels or the pin fins. Based on the nondimensional approach, the Nusselt number is shown to be the inverse of the nondimensional temperature. To examine the thermohydraulic performance, the performance evaluation criterion, PEC, will be calculated, and its formulation is

PEC = $\frac{\mathrm{Nu_{ave}}}{\mathrm{f}^{0.333}}$, where the friction factor f is related to the pressure drop between the inlet and the outlet. Here, f is found equal to $2\frac{\mathrm{D}}{\mathrm{L}}\frac{\Delta\mathrm{P}}{\mathrm{Re}}$. Finally, the amount of heat extracted from the system is known as $\mathrm{Q} = \theta_{out}\cdot\mathrm{Re}\cdot\mathrm{Pr}$ in nondimensional form.

4. Mesh Sensitivity Analysis

Mesh sensitivity analysis is crucial to determine the optimum mesh size for the most accurate results. In COMSOL, different mesh levels are provided and identified by other names. It is mainly extremely coarse, followed by extra coarse, coarser, coarse, normal, fine and finer. It is essential to mention that different problems may need different mesh refinement. In the present context, three divergent channel model is used for the mesh sensitivity. The Reynolds number is fixed to 100, and the average Nusselt number is calculated at the channel's base.

Table 2 presents the analysis summary, and as shown, a "normal" mesh level is acceptable for the numerical analysis. Figure 3 illustrates the mesh size applied to the model. For the complete study, a normal mesh level will be used.

Table 2. Mesh sensitivity.

Mesh Level	Number of Elements	Average Nusselt Number
Extremely Coarse	15,051	1.9431
Extra Coarse	25,769	1.94344
Coarser	46,524	1.97148
Coarse	112,276	1.9664
Normal	214,254	1.961

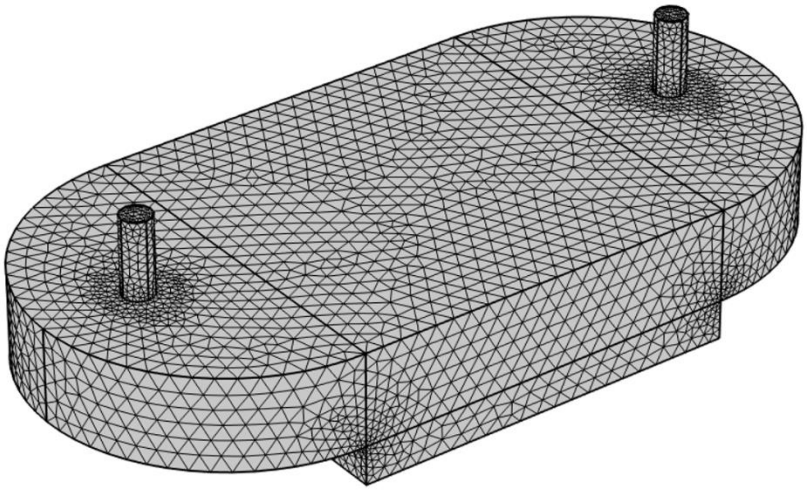


Figure 3. Mesh model.

5. Model Validation with Experimental Data

It is essential to give the reader confidence in the model's accuracy under study by comparing the experimental results obtained by Ho et al. [18] with the numerical model under investigation. Ho et al. [18] experimented by circulating different fluids, including distilled water, through convergent mini channels while the divergent channels were solid, and the heat sink block was heated from the bottom. Eight convergent mini channels were included within a surface area of 50 mm in length and 25 mm in depth. The channel height is 1.5 mm. Figure 4 presents the model under investigation.

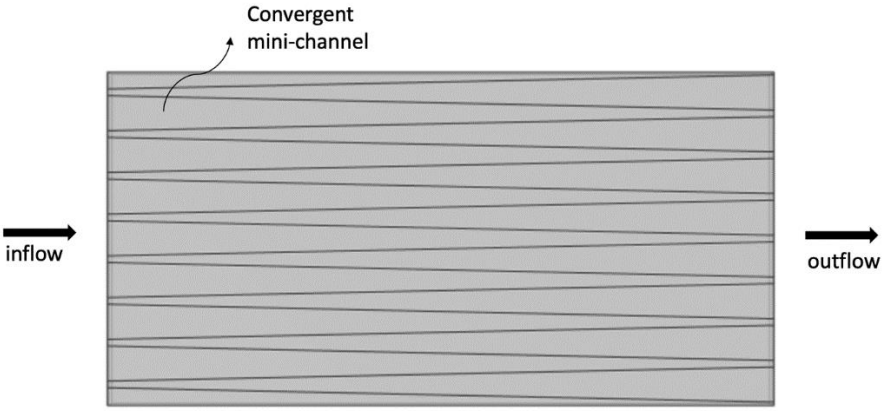


Figure 4. Convergent mini channel model.

The flow enters at a constant temperature, and water circulates through the mini channel and exits from the other end. The nondimensional temperature defined by Ho et al. is measured in the copper block below the water circulation. Figure 5 presents the comparison between the experimental data and numerical results.

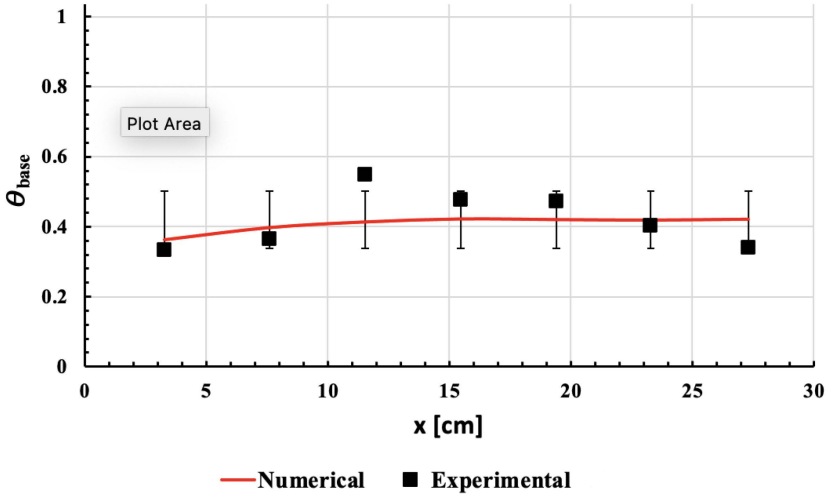


Figure 5. Wall temperature comparison. Experimental [18].

The fluid used for comparison is distilled water, for which the physical properties are well known in the literature. The model was computed for a Reynolds number, according to Ho et al. definition, equal to 90. As shown, the temperature variation pattern is similar, and the trend variation of the temperature along the flow is accurate. The difference between the experimental and numerical data may be due to heat losses and measurement accuracy. It is evident from this comparison that the trend between the experiment and the numerical model is correct. One reason for this discrepancy may be because the fluid particles enter the convergent channel and then they accelerate toward the exit. So, it is believed that the flow regime changes from laminar to transition and further to turbulent regime.

6. Results and Discussion

In this paper, different cases and conditions will be investigated. In the first case, an investigation of the spacing between the pin-fins will be studied, and the best spacing leading to higher heat extraction will be adopted and used in the remaining of the paper for the pin-fins configuration. Secondly, the height of the pin fins and the channel walls will be varied and discussed in detail. All those configurations are in the test section.

6.1. Importance of Spacing between Pin-Fins

Distance spacing in this context, as shown in Figure 1c, is the distance between two pin-fins along the convergent line. Such spacing between pin-fins may influence the flow circulation in the test section. Three cases were studied when the spacing between two pin-fins, as shown in Figure 1c, is 10 mm, 5 mm, and 3.33 mm, respectively. The heating condition, as well as the flow condition, are identical for the three cases under investigation. Since the diameter of the pin-fins is similar to the channel wall thickness, the shorter distance between pin-fins becomes close to the solid wall channels case. The test section used in this case is when the pin-fins form the shape of three convergent/divergent channels.

Figure 6a presents the Nusselt number measured at the base of the pin-fins, where the pin-fins heights are studied for two heights of 2 mm and 6 mm. As shown, for a Reynolds number equal to 100, spacing between two consecutive pin-fins along the convergent or divergent line has no effect. As the flow rate increases (i.e., Re), it is evident that the best pin-fins spacing is when "Sp" is set equal to 10 mm. As the pin-fins height increases and is equal to 6 mm, as shown in Figure 6b, the spacing of 10 mm is still the best option for the design. An identical observation is also detected for a height of 8 mm.

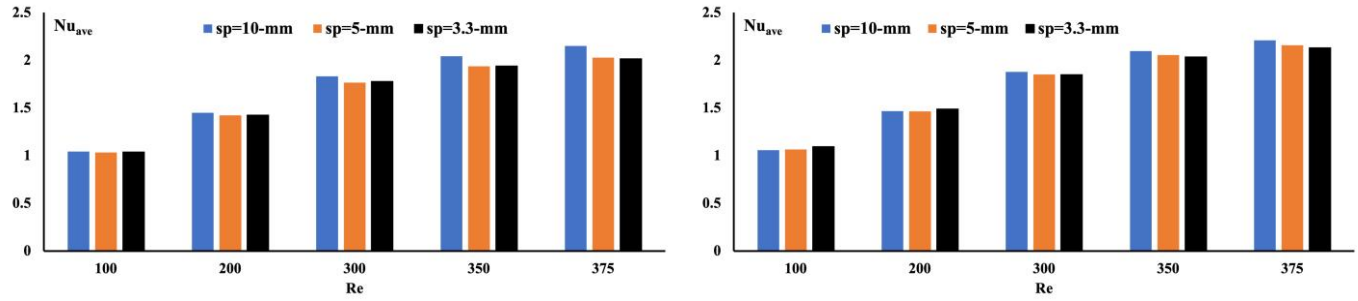


Figure 6. Average Nusselt number for different spacing. (**a**) H = 2 mm (**b**) H = 6-mm.

Another indicator worth mentioning is the Performance Evaluation Criterion (PEC). Figure 7 presents the PEC for the two cases of H = 2 mm and H-6-mm. It is evident from this figure that the most suitable spacing is when "Sp" is equal to 10 mm. For the remaining paper, a spacing of 10 mm will be adopted.

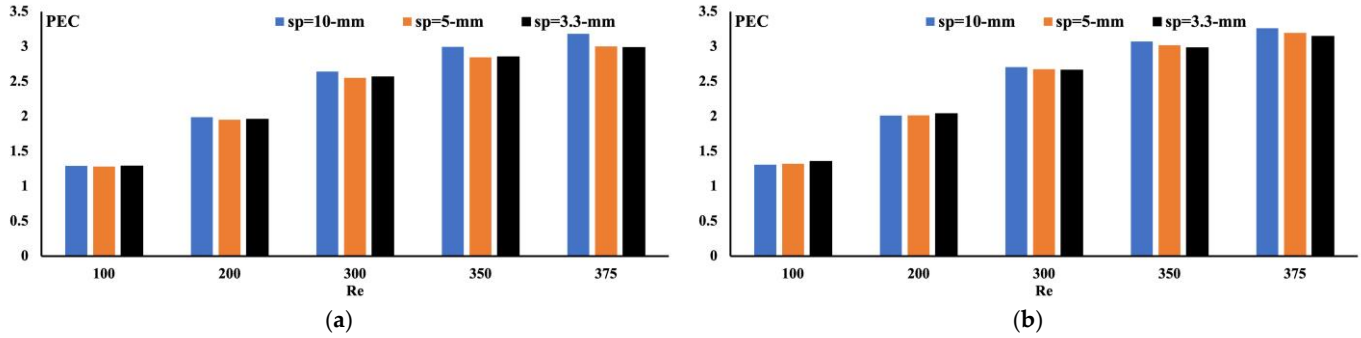


Figure 7. PEC for different spacing (**a**) H = 2 mm (**b**) = H = 6-mm.

6.2. Thermohydraulic Performance of Convergent/Divergent Channels

The seven convergent/divergent channels system is investigated in detail to proceed further with the investigation. The channel heights have varied from 2 mm to 8 mm. Figure 8 shows the channels under investigation in two different views. As shown, free space between the top tip of the channels and the top boundary wall allows the flow to circulate in the channels and above it. The reason for this is that the flow passes through the channels and above the channels, thus creating a mixing for heat enhancement and a reduction in the pressure drop. Figure 8 top view shows that the fluid circulated in the convergent and divergent channels. This is contrary to Ho et al., where the divergent channel was solid. When the fluid passes through the convergent channels, it accelerates along the way. On the contrary, the flow decelerates when the flow goes through the divergent channels. This acceleration and deceleration process help extract heat at a greater rate compared to straight channel configuration.

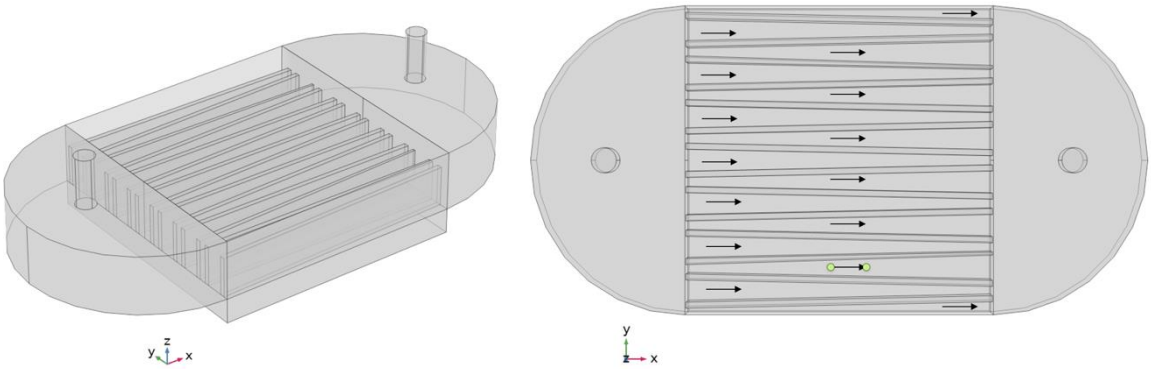


Figure 8. Channels configurations under study.

The model is investigated for Reynolds numbers 100, 200, 300, 350 and 375, respectively. The heights, as indicated earlier, vary from 2 mm to 8 mm with an increment of 2 mm. Figure 9 presents the variation of the average Nusselt number as a function of the Reynolds number.

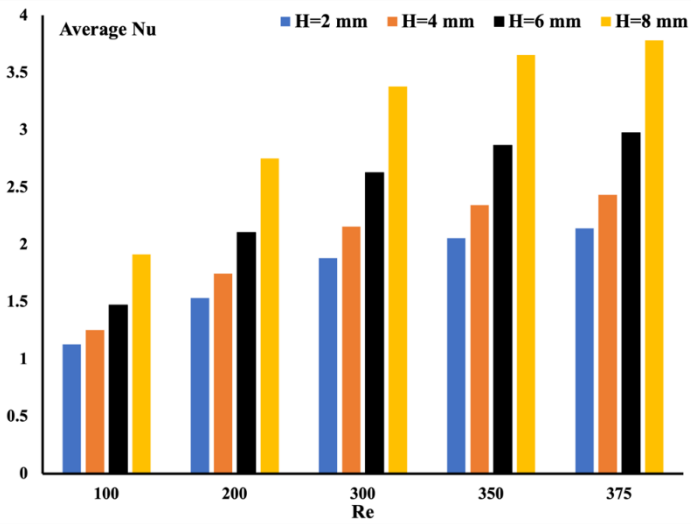


Figure 9. Average Nusselt number (Seven Channels configurations).

Two interesting findings could be drawn from these results. The first is that when the channel's height is 8 mm, an intense mixing occurs at a low Reynolds number due to a high Nusselt number. This leads to a more pronounced heat extraction. The second finding is that as the Reynolds number increase, the heat enhancement increases accordingly, and the best configuration is when the channel height is 8 mm. This finding could be further investigated by calculating the performance evaluation criterion, shown in Figure 10.

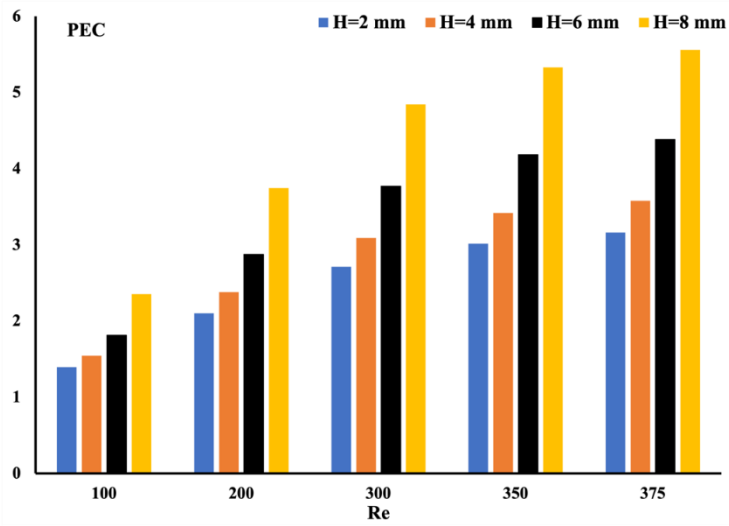


Figure 10. PEC for Convergent/Divergent channels (Seven Channels configurations).

Since the performance evaluation criterion is the ratio of the average Nusselt number to the friction to the power 0.333, the earlier observation is valid in this figure. The PEC is found to be higher for a channel of 8 mm in height for all ranges of Reynolds number. Thus, mixing may also directly affect this parameter since the pressure drop in all cases was found to be equally low. Since we aim to investigate the best heat enhancement, Figure 11 evaluates the amount of heat extracted from the system. Here, it is evident that the 8 mm channel height removed more heat from the system; however, as the Reynolds number increases, heat transfer into the fluid decreases.

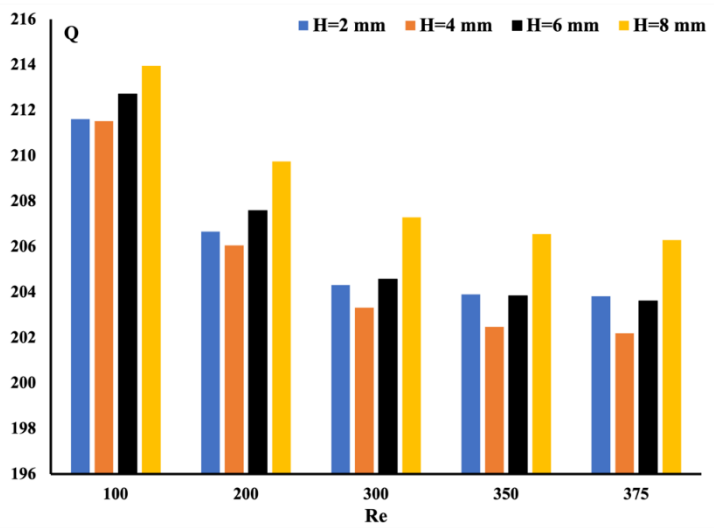
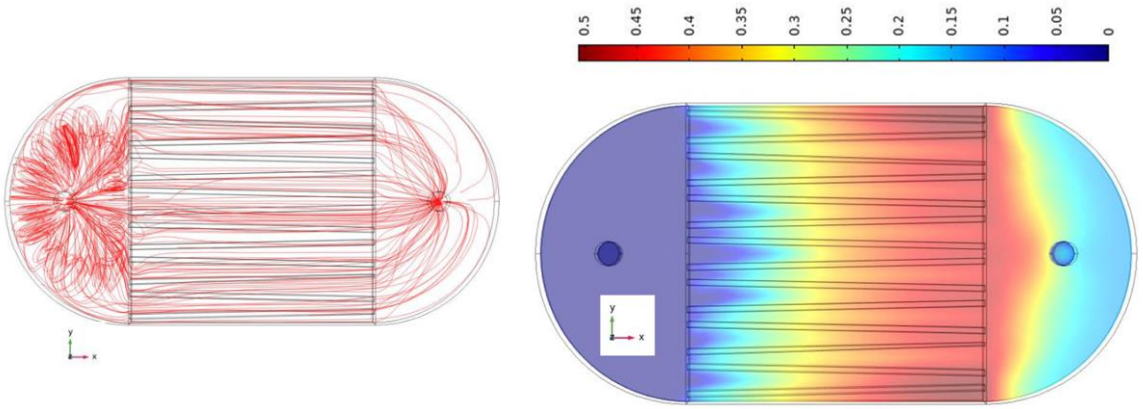


Figure 11. Heat extracted from the system (Seven Channels configurations).

One may conclude here that convergent/divergent channels achieve high heat extraction and the best case is when the height of the channel is 8 mm. That means the flow between channels and above channels helps create mixing leading to better heat extraction.

A more appropriate way to study the flow inside the test section is to examine the flow and temperature profile at the (x,y) plane, as shown in Figure 12. The iso-stream line shown in Figure 12a indicates two types of circulations. The first is the flow passing through the convergent/divergent channels, and the second is the flow circulating above the channels since the channel height is 8 mm and the test section height is 12 mm. Many rotating flows are observed within the mixing chamber before entering the channels. These rotating cells are due to the location of the fluid injector. Figure 12b shows the temperature profile for

the same condition. As shown at the channel's entrance, the flow starts absorbing heat, and as the flow accelerates in the convergent channel, more cooling occurs. Contrary to the divergent channels, the cooling is weak at the end and very pronounced at the entrance. Most of the cooling occurs toward the end of the flow.



(**a**) (**b**)

Figure 12. Velocity and temperature distribution for Re = 300. (**a**) Velocity; (**b**) Temperature.

6.3. Thermohydraulic Performance of Pin-Fins Channels

In the previous study by the author [26], pin-fins straight channels performed better than regular straight channels with walls. This observation is because the pin-fins absorbed more heat, allowing the flow to circulate between pin-fins and reducing the pressure drop between the inlet and the outlet. Here, the channel walls were replaced with pin-fins spaced by 10 mm, allowing the flow to circulate freely on the hot surface. In Section 6.1, we have demonstrated that the best performance occurs when the spacing between the pin-fins is 10 mm.

Figure 13 presents the average Nusselt number calculated at the base of the pin-fins, like in the previous cases. The model was investigated for different flow rates corresponding to different Reynolds numbers. As the Reynolds number increases, the heat removal or enhancement represented by the Nusselt number increase, respectively. However, it is evident that with 8 mm pin-fins heights, the average Nusselt number is more pronounced. Pin-fins with 2 mm heights showed the lowest heat enhancement but were still very close to 8 mm pin-fins height.

It is also observed that the pin-fins height of 2 mm outperformed the 4 mm and the 6 mm pin-fins. There must be a reason for this to happen. Since, for all cases, the pressure drops and thus the friction coefficient exhibited a similar level, the performance evaluation criterion shown in Figure 14 showed a similar finding to Figure 13. In conclusion, the pin-fins with a height of 8 mm showed the best performance for heat enhancement, followed by the 2 mm pin-fins height. The amount of heat absorbed by the fluid is calculated by measuring the outlet temperature and is related to the Reynolds number. As the Reynolds number increases, less time is allocated for the heat to be absorbed, thus lower heat transferred to the fluid. Figure 15 presents the amount of heat extracted.

It is interesting to notice that the lower pin-fins height may have created more mixing. The heat transferred to the circulating fluid is slightly greater than in the other cases. This finding justifies that as the Reynolds number increases, the mixing is more pronounced. Figure 16 presents the fluid circulation and the temperature distribution for the case of Reynolds number equal to 300, and the pin-fins height is 8 mm.

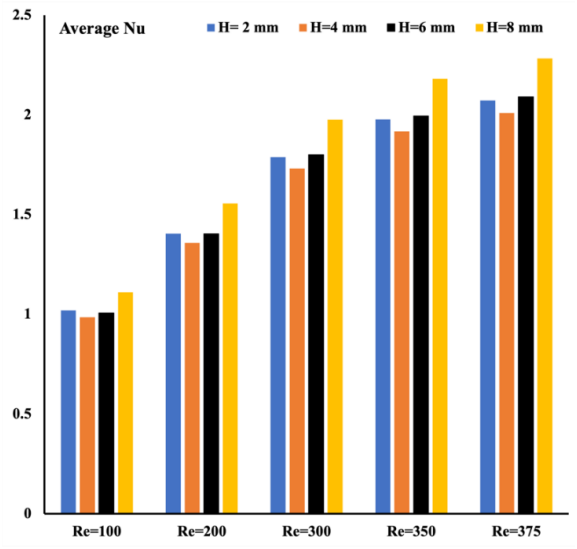


Figure 13. Average Nusselt number (Seven pin-fins channel configurations).

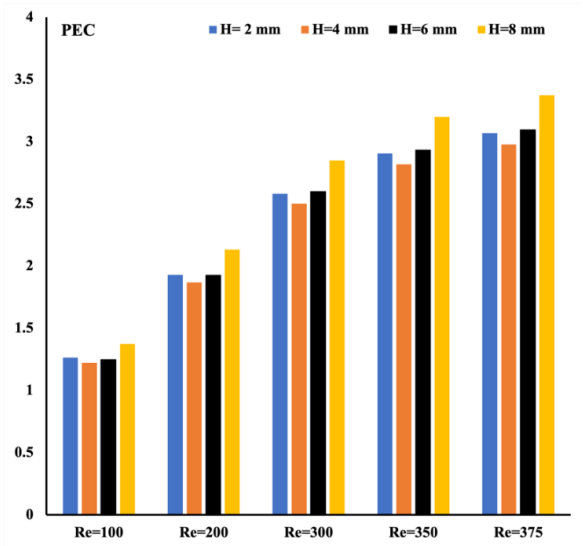


Figure 14. PEC for Convergent/Divergent channels (Seven pin-fins channel configurations).

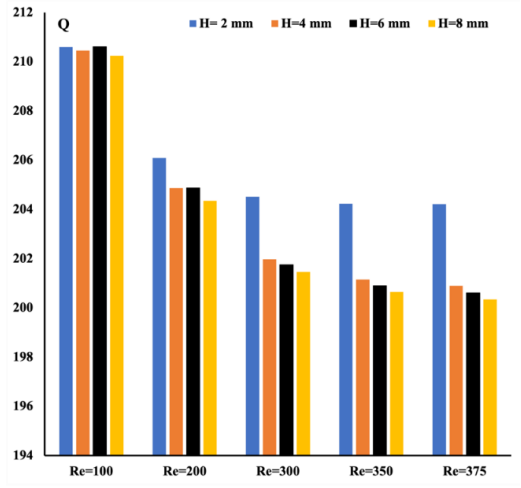
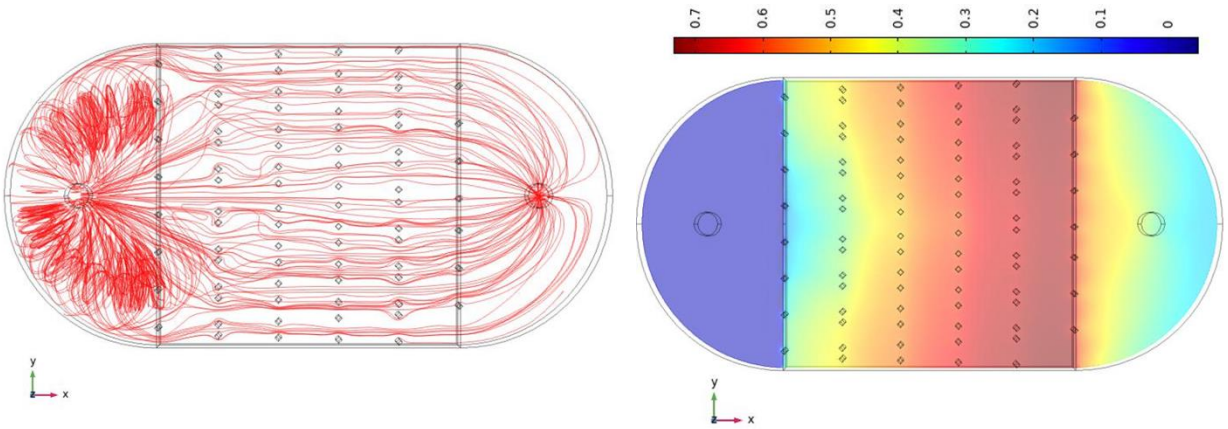


Figure 15. Heat extracted from the system (Seven pin-fins channel configurations).



(**a**) (**b**)

Figure 16. Iso-streamlines and temperature distribution for Re = 300. (**a**) Iso-streamlines, (**b**) Temperature variation (Pin-fins height 8 mm).

By observing Figure 16, the pin-fins structure in a convergent/divergent channel does not affect heat removal, followed by the channel's configuration. Additionally, by examining the temperature distribution, it is evident that the channel configuration provided a more noticeable cooling effect than the pin-fins configuration. In Figure 16, the flow circulated between the pin-fins and above, not taking advantage of the convergent/divergent structure.

7. Conclusions

In the present paper, an attempt is made to investigate the effectiveness of using convergent/divergent channels and compare them to pin similar fin structures. Both cases had an identical mass of aluminum and equal height. It is observed that;

1. The convergent/divergent channels provided an enhanced flow circulation leading to better heat enhancement.
2. The convergent channels are more effective than the divergent channel. The reason for this is the accelerating flow near the end where the heat is accumulated.
3. Although pin-fins help extract heat, the proposed shape did not add to the heat enhancement.
4. The flow circulated more freely between the pin-fins.
5. Because the heights of the channels and pin-fins were lower than the cavity height, the pressure drop was minimal.
6. The flow above the channels/pin-fins and between them created a mixing which helped heat extraction.

Funding: The author acknowledges the funding by the National Science and Engineering Research Canada (NSERC).

Data Availability Statement: Not applicable.

Conflicts of Interest: No conflict of interest.

Nomenclature

D	Hydraulic diameter [m]
x,y,z	Dimensions [m]
u_{in}	Inlet velocity [m/s]
u,v,w	Velocities [m/s]
p	Pressure [Pa]
q″	Heat flux [W/m^2]
T_{in}	Inlet temperature [K]
k	Fluid conductivity [W/m/K)
C_p	Fluid specific heat [J/kg/K]
PEC	Performance evaluation criterion
H	Pin-fins height [mm]
sp	Space between pin-fins [mm]
Non-dimensional parameters	
X,Y,Z	Dimensions
U,V,W	Velocities in X,Y,Z
P	Pressure
Re	Reynolds number
θ_{out}	Outlet temperature
Nu	Nusselt number
Pr	Prandtl number
Q	Heat absorbed by the fluid
$\Delta P = P_{in} - P_{out}$	Pressure drop
f	Friction factor
Greek letters	
θ	Temperature
μ	Viscosity [kg/m/s]
ρ	Density [kg/m^3]
τ	Time

References

1. Srivastava, P.; Dewan, A.; Bajpai, J.K. Flow and heat transfer characteristics in convergent-divergent shaped microchannel with ribs and cavities. *Int. J. Heat Technol.* **2017**, *35*, 863–873. [CrossRef]
2. Srivastava, P.; Dewan, A. A study of turbulent heat transfer in convergent-divergent shaped microchannel with ribs and cavities using CFD. *J. Mech. Eng. Sci.* **2020**, *14*, 6344–6361. [CrossRef]
3. Duryodhan, V.S.; Singh, A.; Singh, S.G.; Agrawal, A. Convective heat transfer in diverging and converging microchannels. *Int. J. Heat Mass Transf.* **2015**, *80*, 424–438. [CrossRef]
4. Lee, M.S.; Jeong, S.S.; Ahn, S.W.; Han, J.C. Effects of angled ribs on turbulent heat transfer and friction factors in a rectangular divergent channel. *Int. J. Therm. Sci.* **2014**, *84*, 1–8. [CrossRef]
5. Bayomy, A.M.; Saghir, Z. Thermal performance of finned aluminum heat sink filled with ERG aluminum foam: Experimental and numerical approach. *Int. J. Energy Res.* **2020**, *44*, 4411–4425. [CrossRef]
6. Rahman, M.M.; Saghir, Z.; Pop, I. Free convective heat transfer efficiency in Al_2O_3–Cu/water hybrid nanofluid inside a rectotrapezoidal enclosure. *Int. J. Numer. Methods Heat Fluid Flow* **2021**, *32*, 196–218. [CrossRef]
7. Yang, X.H.; Tan, S.C.; Ding, Y.J.; Liu, J. Flow and thermal modeling and optimization of micro/mini-channel heat sink. *Appl. Therm. Eng.* **2017**, *117*, 289–296. [CrossRef]
8. Mokrani, O.; Bourouga, B.; Castelain, C.; Peerhossaini, H. Fluid flow and convective heat transfer in flat microchannels. *Int. J. Heat Mass Transf.* **2009**, *52*, 1337–1352. [CrossRef]
9. Plant, R.D.; Saghir, M.Z. Numerical and experimental investigation of high concentration aqueous alumina nanofluids in a two and three channel heat exchanger. *Int. J.* **2021**, *9*, 100055. [CrossRef]
10. Gorzin, M.; Ranjbar, A.A.; Hosseini, M.J. Experimental study on serpentine minichannel heat sink: Effect of rib existence and distance. *Int. J. Therm. Sci.* **2022**, *173*, 107397. [CrossRef]
11. Xie, X.L.; Liu, Z.J.; He, Y.L.; Tao, W.Q. Numerical study of laminar heat transfer and pressure drop characteristics in a water-cooled minichannel heat sink. *Appl. Therm. Eng.* **2009**, *29*, 64–74. [CrossRef]
12. Vajravel, L.V.; Swaminathan, S.K.; Baskaran, S.; Sekar, R.K. Experimental investigations on heat transfer in a new minichannel heat sink. *Int. J. Therm. Sci.* **2019**, *140*, 144–153. [CrossRef]
13. Begag, A.; Saim, R.; Öztop, H.F.; Abboudi, S. Numerical Study on Heat Transfer and Pressure Drop in a Mini-Channel with Corrugated Walls. *J. Appl. Comput. Mech.* **2021**, *7*, 1306–1314.

14. Khoshvaght-Aliabadi, M.; Sahamiyan, M.; Hesampour, M.; Sartipzadeh, O. Experimental study on cooling performance of sinusoidal–wavy minichannel heat sink. *Appl. Therm. Eng.* **2016**, *92*, 50–61. [CrossRef]
15. Khoshvaght-Aliabadi, M.; Feizabadi, A.; Nouri, M. Design of novel geometries for minichannels to reduce junction temperature of heat sinks and enhance temperature uniformity. *Appl. Therm. Eng.* **2021**, *192*, 116926. [CrossRef]
16. Khoshvaght-Aliabadi, M.; Hosseinirad, E.; Farsi, M.; Hormozi, F. Heat transfer and flow characteristics of novel patterns of chevron minichannel heat sink: An insight into thermal management of microelectronic devices. *Int. Commun. Heat Mass Transf.* **2021**, *122*, 105044. [CrossRef]
17. Wan, Z.; Lin, Q.; Wang, X.; Tang, Y. Flow characteristics and heat transfer performance of half-corrugated microchannels. *Appl. Therm. Eng.* **2017**, *123*, 1140–1151. [CrossRef]
18. Ho, C.J.; Liu, Y.C.; Yang, T.F.; Ghalambaz, M.; Yan, W.M. Convective heat transfer of nano-encapsulated phase change material suspension in a divergent minichannel heatsink. *Int. J. Heat Mass Transf.* **2021**, *165*, 120717. [CrossRef]
19. Sohel, M.R.; Khaleduzzaman, S.S.; Saidur, R.; Hepbasli, A.; Sabri, M.F.; Mahbubul, I.M. An experimental investigation of heat transfer enhancement of a minichannel heat sink using Al2O3–H2O nanofluid. *Int. J. Heat Mass Transf.* **2014**, *74*, 164–172. [CrossRef]
20. Ijam, A.; Saidur, R.; Ganesan, P. Cooling of minichannel heat sink using nanofluids. *Int. Commun. Heat Mass Transf.* **2012**, *39*, 1188–1194. [CrossRef]
21. Ho, C.J.; Chen, W.C. An experimental study on thermal performance of Al_2O_3/water nanofluid in a minichannel heat sink. *Appl. Therm. Eng.* **2013**, *50*, 516–522. [CrossRef]
22. Ho, C.J.; Liao, J.C.; Li, C.H.; Yan, W.M.; Amani, M. Experimental study of cooling performance of water-based alumina nanofluid in a minichannel heat sink with MEPCM layer embedded in its ceiling. *Int. Commun. Heat Mass Transf.* **2019**, *103*, 1–6. [CrossRef]
23. Ho, C.J.; Chen, W.C.; Yan, W.M. Experimental study on cooling performance of minichannel heat sink using water-based MEPCM particles. *Int. Commun. Heat Mass Transf.* **2013**, *48*, 67–72. [CrossRef]
24. Ghasemi, S.E.; Ranjbar, A.A.; Hosseini, M.J. Experimental evaluation of cooling performance of circular heat sinks for heat dissipation from electronic chips using nanofluid. *Mech. Res. Commun.* **2017**, *84*, 85–89. [CrossRef]
25. Awais, A.A.; Kim, M.H. Experimental and numerical study on the performance of a minichannel heat sink with different header geometries using nanofluids. *Appl. Therm. Eng.* **2020**, *171*, 115125. [CrossRef]
26. Saghir, M.Z.; Rahman, M.M. Thermo-Hydraulic Performance of Pin-Fins in Wavy and Straight Configurations. *Micromachines* **2022**, *13*, 954. [CrossRef] [PubMed]